Gerard Caneba

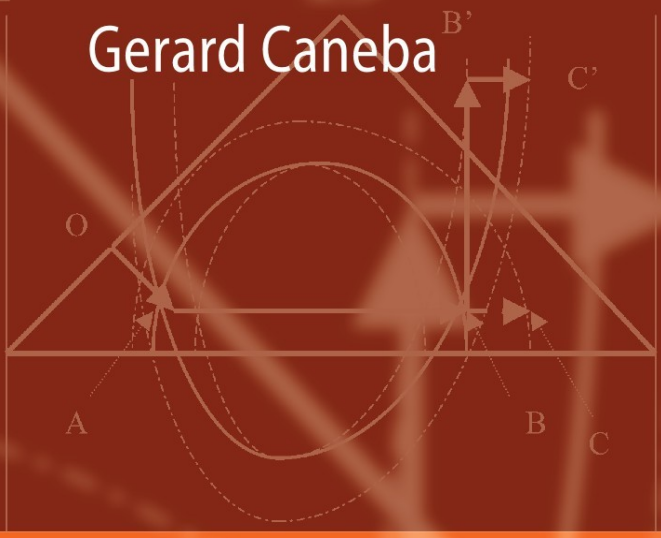

Free-Radical Retrograde-Precipitation Polymerization (FRRPP)

Novel Concept, Processes, Materials, and Energy Aspects

Springer

Free-Radical Retrograde-Precipitation Polymerization (FRRPP)

Gerard Caneba

Free-Radical Retrograde-Precipitation Polymerization (FRRPP)

Novel Concept, Processes, Materials, and Energy Aspects

Springer

Dr. Gerard Caneba
Michigan Technological
University
Dept. Chemical Engineering
1400 Townsend Drive
Houghton MI 49931-1295
USA
caneba@mtu.edu

ISBN 978-3-642-03024-6 e-ISBN 978-3-642-03025-3
DOI 10.1007/978-3-642-03025-3
Springer Heidelberg Dordrecht London New York

Library of Congress Control Number: 2009937716

Cover design: WMXDesign GmbH, Heidelberg

Printed on acid-free paper

Springer is part of Springer Science+Business Media (www.springer.com)

Dedicated to my loving wife, Mary Ann; my children, Christine, Richard, Benjamin, and Katherine; and to my parents, Doroteo and Saturnina Cañeba

Preface

The free-radical retrograde-precipitation polymerization (FRRPP) process was introduced by the author in the early 1990s as a chain polymerization method, whereby phase separation is occurring while reactive sites are above the lower critical solution temperature (LCST). It was evident that certain regions of the product polymer attain temperatures above the average fluid temperature, sometimes reaching carbonization temperatures. During the early stages of polymerization-induced phase separation, nanoscale polymer domains were also found to be persistent in the reacting system, in apparent contradiction with results of microstructural coarsening from constant-temperature modeling and experimental studies. This mass confinement behavior was used for micropatterning, for entrapment of reactive radical sites, and for the formation of block copolymers that can be used as intermediates, surfactants, coatings, coupling agents, foams, and hydrogels. FRRPP-based materials and its mechanism have also been proposed to be relevant in energy and environmentally responsible applications.

This technology lacks intellectual appeal compared to others that have been proposed to produce polymers of exotic architectures. There are no special chemical mediators needed. Control of conditions and product distribution is done by process means, based on a robust and flexible free-radical-based chemistry. Thus, it can readily be implemented in the laboratory and in production scale.

The FRRPP process is what the author calls a third-world method to produce multipolymers; and having spawned from the developing world, the author writes this monograph in appreciation of his beginnings that led to a life of discovery in new worlds. As for developed countries, this monograph offers insights into future energy independence and frontier intellectual explorations. It is not to say that the developed world can just sit on these insights; as the nature of the FRRPP technology suggests, even these advanced ideas can be exploited by others of limited resources.

This monograph contains a new dimensionless quantity, which the author believes to contain the sufficient-and-necessary condition for FRRPP behavior. It is symbolized as $C\tilde{n}$ (pronounced see-enye) and introduced in Section 2.2. In order to assure strict FRRPP behavior, computer simulation has established $C\tilde{n}$ to be less than -1000. This cutoff number could definitely be changed, if certain criteria for strict FRRPP behavior are relaxed. Experimental measurements seems to indicate

that *Cñ* should be a large enough negative number. The *Cñ* designation for the new dimensionless number is made in honor of the author's extended family name and Filipino–Hispanic heritage.

The FRRPP process involves a novel synergistic combination of various concepts. The author does not claim mastery of state-of-the-art understanding of the various fields it encompasses. He believes that even if these subareas may be imperfectly understood, the combination can yield novel discoveries. Over the history of science and technology, important discoveries were made this way. This is related to the recent discoveries of better performance from a group of persons of diverse backgrounds and perspectives working in a team or organization, even though individually they may not be the best in their positions.

Gratitude is expressed to Michigan Technological University for providing the intellectual atmosphere and isolation, as well as the pristine environment to carry out the research efforts that facilitated the development of the FRRPP concept. Crucial funding from various agencies and foundations are also appreciated, especially the National Science Foundation through Maria Burka of the Process Reaction Engineering Program and Norbert Bikales of the Polymers Program at the Division of Materials Research.

A significant amount of material from this monograph has been generated through the efforts and assistance of the author's former graduate and undergraduate students, post-doctoral associates, co-investigators in various projects involving the FRRPP process, and other supporters. The list includes Yadunandan Dar, Bo Wang, Rahul Saxena, Vijay Tirumala, Yi Zhao, Linhuo Shi, Anand Laxminarayan, Yuh-Ling Chen, Zhiyong Xu, Yuhao Cai, Anuj Aggarwal, Brian Ott, Michael Renier, Derrick Mancini, Douglas Gardner, Stephen Shaler, Pete Schlom, David Shonnard, Ghatu Subhash, David Johnson, Brooke Hatfield, Mitchell Zakin, Karel Solc, Jay Axland, Michael Crossey, Ahmed Bahabry, and many more with relatively minor roles. The author would also like to express appreciation to his mentors at the University of California – Berkeley: John Prausnitz, David Soong (now Soane), and Morton Denn, for all the intellectual discussions with them as a wide-eyed and inquisitive graduate student. A final gratitude is expressed to the University of the Philippines and UNESCO for providing the author the opportunity to start his studies in the United States.

The foregoing material in this monograph starts with background material in Chapter 1, which introduces the reader to the various components of the FRRPP process: phase equilibria thermodynamics, transport processes, phase separation kinetics, free-radical polymerization, and reactive phase separation. Then, in Chapter 2, the author introduces the FRRPP process and its various features. In Chapter 3, the FRRPP process is applied to polymerization processes, including statistical multipolymerizations and staged block copolymer formation. In Chapter 4, various applications of the FRRPP process developed by the author within his research group are presented. In Chapter 5, the author presents some of the energy-related applications of the FRRPP process, as they relate to his work in enhanced oil recovery. Finally, Chapter 6 involves a discussion of some future and more speculative uses of the FRRPP process and its conceptual underpinnings, in relation to nanotechnology, medical research, and control over other forms of energetic systems. It is suggested

that readers scan through the background material in Chapter 1 in order to obtain at least a cursory understanding of conventional fields related to the FRRPP process, before they embark on a reading adventure of the latter chapters. If there are problems understanding material beyond Chapter 1, careful reading of the background chapter (including some of the cited references) would be the required.

For those who are seasoned and practitioners in the field of polymerization processes, starting in Chapter 2 or even Chapter 3 could be worth the try. For technologists whose interest in this material is confined to products and applications, jumping into Chapter 4 onward could serve its purpose. For students of the art and science of polymer and energetic systems, it is a hope that their intellectual horizons will become more open after reading and absorbing the various ideas contained in this monograph.

Houghton, Michigan USA Gerard T. Caneba
September 2009

Contents

Chapter 1
Background

An adequate understanding of the FRRPP process can never be achieved without probing into its underlying concepts, since it is a synergistic combination of thermodynamic, transport, and polymer chain-reaction kinetics. The overall result is an unconventional polymerization and energetic behavior that requires the conceptual and mathematical understanding to link all FRRPP features into a coherent picture. Since its necessary condition is found in a phase behavior of polymer mixtures under equilibrium conditions, it is appropriate that the start of presentation of the technical aspects of the FRRPP process is in its relevant thermodynamic concepts.

Phase diagrams of polymer/small-molecule systems are used to determine concentrations or compositions of uniform phases (liquids or solids) at equilibrium. Equilibrium in the thermodynamic sense means that conditions of temperature, pressure, and component compositions do not change with time at a scale much larger than molecular dimensions. Also, the mixture is either a closed system or a representative sample of an overall system. If the system is made up of two components (i.e., a binary system), a typical phase diagram shown in Fig. 1.1.1(a) could have a lower concave-down curve and an upper concave-up curve in the composition–temperature plot (Saeki et al., 1973). The maximum of the concave-down curve is the upper critical solution temperature (UCST), whereas the minimum of the concave-up curve is the lower critical solution temperature (LCST). Outside the concave curves represents single-phase mixtures, just like honey or wine. Shaded regions inside the concave perimeter curves are areas that correspond to mixtures that permit coexistence of two phases. This means that immiscibility can occur if the temperature of the polymer solution is raised above the LCST or lowered below the UCST. The UCST and LCST envelopes display a roughly mirror-image view of each other (Casassa and Berry, 1989). By increasing the molecular weight of the polymer, the UCST is raised and LCST is lowered, thus shrinking the temperature region of complete miscibility. If a solvent of poor quality is chosen, the increase of molecular weight could cause the UCST and LCST to overlap, so that the two regions of limited miscibility merge into an hourglass-shape phase envelope (Siow et al., 1972) (Fig. 1.1.1(b)).

The LCST behavior has long been known to occur in polar small-molecule and polymer/small-molecule systems, and these temperatures can be close to room

G. Caneba, in: *Free-Radical Retrograde-Precipitation Polymerization (FRRPP)*,
Chapter DOI 10.1007/978-3-642-03025-3_1,

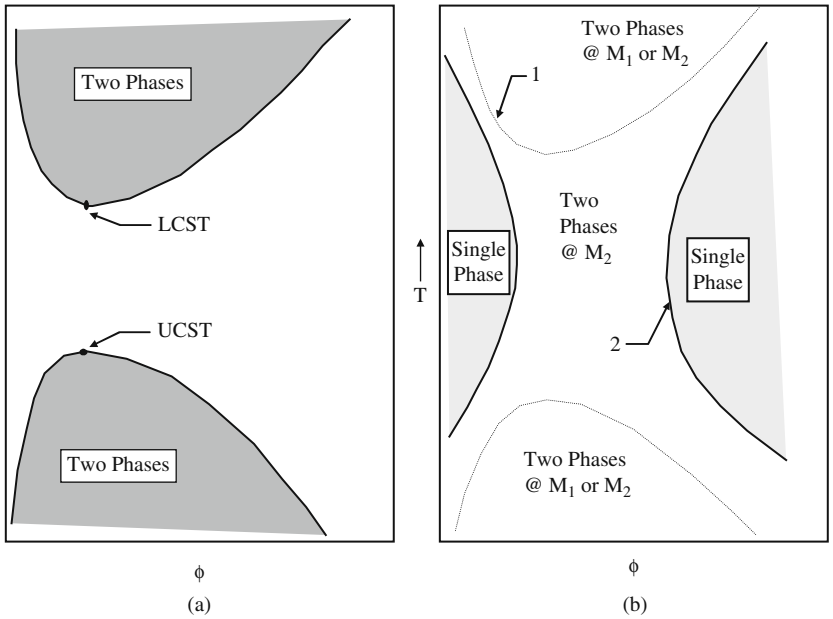

Fig. 1.1.1 Binary phase diagrams (polymer composition represented by the volume fraction, ϕ, vs temperature, T) of polymer/solvent systems exhibiting: (**a**) both LCST and UCST phase envelopes and (**b**) the hourglass-shape phase behavior, when the polymer 2 molecular weight is greater than that of polymer 1 (or $\bar{M}_2 > \bar{M}_1$)

temperature at or around atmospheric pressure. It has not been too long since nonpolar systems were first found to exhibit LCST behavior (Freeman and Rowlinson, 1960), although for most part it occurs at elevated temperatures and pressures. From a practical standpoint, it would be better if LCST values of nonpolar systems are close to small-molecule boiling temperatures; however, more and more data indicate that these values are closer to small-molecule critical temperatures instead. For nonpolar polymer/small-molecule systems, results seem to indicate that the LCST behavior is more of a rule than an exception (Saeki et al., 1973) and that usually there would also be UCST behavior. In fact, there have been cases wherein these systems may not show UCST behavior at all, because small-molecule components are good solvents for the polymer (Casassa and Berry, 1989). Thus, the LCST phenomenon may be quite unusual, but it is a prevalent behavior in polymer/small-molecule systems. It is just a matter of finding the right solvent or mixed solvent combination in the polymer one would like to work with.

From a molecular standpoint, the LCST behavior can be attributed to (**a**) strong polar interactions, including hydrogen-bonding interactions; and, (**b**) equation-of-state (compressibility) effects. In both cases, LCST phase separation is entropically driven (Sanchez and Panayiotou, 1993). Whenever strong interactions are important, they will decrease the entropy more than non-strong interactions,

because strong interactions induce more spatial orientation. At low temperatures, the potential energy gain in strong interactions offset the unfavorable entropy change. As the temperature increases, the unfavorable entropy change becomes more important and finally induces the LCST phase separation when this entropy change overwhelms the favorable energy change. In a nonpolar system, finite compressibility or equation-of-state effects dominate the LCST behavior. At high enough temperatures, unfavorable entropy changes associated with the densification of the mixture become prohibitive for a single-phase system (Sanchez and Panayiotou, 1993). Patterson et al. (1967) reported that the ratio of LCST-to-small-molecule critical temperature for many polyethylene (PE), polyisobutylene (PIB) and polydimethylsiloxane (PDMS) solutions with *n*-alkanes, lies between 0.8 and 0.98 K/K because of the difference in free volumes between the solvent and the polymer (Patterson, 1969; Somcynsky, 1982). Charlet and Delmas (1981) studied the LCST behavior for ethylene–propylene copolymer (EPM) in a wide range of solvents and found that for C_6 and C_7 alkanes, the LCST is 20–80°C less than the solvent critical temperature. They also correlated the LCST with the solvent density and solvent shape. The same results were obtained by Irani (1986) with both single solvent and mixed solvents for the EPM system. To lower the LCST, Irani et al. (1980) showed that dissolving a low-molecular weight hydrocarbon gas, such as ethylene or propylene, in an EPM solution considerably reduces the LCST. This makes the above explanation about the LCST more reasonable, because usually critical temperatures of low-molecular weight gases are much lower, and the system with such mixed solvents will be expected to show a lower LCST. For some systems, e.g., the PS/acetone solution, an hourglass-shape phase diagram was encountered at relatively high polymer molecular weight (Siow et al., 1972; Saeki et al., 1973). If specific energetic interactions were present (such as PEG/water solutions), a closed-loop behavior may be observed, where the LCST was found below the UCST (Casassa and Berry, 1989).

The fact that the LCST of nonpolar polymer/solvent systems was observed under pressure and close to the solvent critical temperature seemed to be a hindrance to its study and application. Phase separation above the LCST of polymer solution was first applied to the recovery of polymers produced from solution polymerization by Anolick and Goffinet (1966). Although this method potentially involved lower energy requirements compared to conventional solvent evaporation techniques, such as steam stripping, there were limitations for this technique to be widely adopted by industry. One of them was the relatively high LCST values for most of the systems. The addition of a low molecular weight gas into the system did not seem to be attractive enough because of the added component and the resulting increase in operating pressure. A more effective approach was the use of mixed solvents, especially polar and/or hydrogen-bonded types. For example, for polystyrene (PS), the LCST in *t*-butyl acetate was at around 98°C. However, with the addition of a small amount of water (1–2 wt% in the mixture), the LCST was lowered to around 55°C. In the various examples mentioned in this monograph, the reader will get a better sense of the various mixed solvents used in practical FRRPP systems.

1.1 Phase Separation Thermodynamics

The central thermodynamic quantity of interest to characterize phase separation behavior of polymer systems is the Gibbs free energy, G. In turn, the Gibbs free energy is related to the enthalpy, H, and the entropy, S, through the definition

$$G \equiv H - TS. \tag{1.1.1}$$

The enthalpy is associated with the energetic level of the system, while the entropy is related to the level of randomness of the system. Since the absolute Gibbs free energy cannot be determined, its relative value ΔG is used in various calculations and mathematical expressions. When the Gibbs free energy is relative to the weighted mole-average of those of the pure components that make up the mixture, it corresponds to the Gibbs free energy of mixing, ΔG_{M}. Thus,

$$\Delta G_{\mathrm{M}} \equiv G - \sum_i n_i G_{\mathrm{Pure}i}, \tag{1.1.2}$$

where G is the Gibbs free energy of the mixture and n_i is the number of moles of component i.

1.1.1 Thermodynamics of Polymer Solutions

Model equations that characterize component solubilities and phase compositions of polymer solutions range from simpler ones, such as the Flory–Huggins (FH) theory (Flory, 1942; Huggins, 1942), to more complicated ones based on equation-of-state (EOS) models (Prigogine, 1957; Flory, 1970; Patterson, 1968, 1982; Patterson and Delmas, 1970) and lattice fluid models (Sanchez and Lacombe, 1976, 1978; Panayiotou and Vera, 1982; High and Dinner, 1990). At the extreme end of the sophistication are complicated models, such as the Universal Quasi-Chemical or UNIQUAC (Prausnitz et al., 1986), Universal Functional Group Activity or UNIFAC (Fredenslund et al., 1977), perturbed hard sphere chain or PHSC (Prausnitz et al., 1986), and statistical associating fluid theory or SAFT (Condo and Radosz, 1996)]. In this monograph, only the Flory–Huggins and Flory–Prigogine–Patterson equation-of-state theories are presented, since they were the only ones used in subsequent computational efforts.

1.1.1.1 Flory–Huggins Theory

For a binary polymer–solvent solution, the simplest expression for the Gibbs free energy of mixing is based on the Flory–Huggins Theory (Flory, 1942; Huggins, 1942),

$$\Delta G_{\mathrm{M}} = RT\left[n_{\mathrm{S}} \ln \phi_{\mathrm{S}} + n_{\mathrm{P}} \ln \phi_{\mathrm{P}} + n_{\mathrm{S}} \phi_{\mathrm{P}} \chi\right], \tag{1.1.3}$$

where ϕ_P are ϕ_S the volume fractions of the polymer and solvent, respectively. The quantity χ is a dimensionless Flory–Huggins parameter and is initially assumed to be temperature dependent only. Note that Eq. (1.1.3) assumes that the polymer has at least a relatively narrow molecular weight distribution. There are extensions of the Flory–Huggins theory for polydisperse polymers (Guggenheim, 1952; Koningsveld, 1968a, 1968b), but they will not be needed for application to the FRRPP process, since products from the reaction system tend to be relatively narrow in their molecular weight distributions.

The original Flory–Huggins equation represents many of the essentials of polymer solution equilibria, but it is often not able to give a quantitative representation of experimental data. Some of the critical assumptions made for its development are (a) random mixing, i.e., polymer segments and solvent molecules show no preference in choosing nearest neighbors; and (b) rigid lattice without holes.

For a mixture that is applicable to the FRRPP process, one can write the multicomponent Flory–Huggins equation as

$$\frac{\Delta G_M}{N_r kT} = \sum_{i=1}^{n} \frac{\phi_i}{r_i} \ln \phi_i + \sum_{j=2}^{n} \sum_{i=1}^{j-1} g_{ij} \phi_i \phi_j, \tag{1.1.4}$$

where N_r is the total number of sites in the lattice and

$$N_r = \sum_i N_i r_i.$$

The quantity g_{ij} is the binary interaction parameter between species i and j and $g_{ij} = g_{ij}$ (T, P, r_i *or* r_j, ϕ_i *or* ϕ_j). The quantity ϕ_i is the volume fraction of component i with $\phi_i = N_i r_i / N_r$.

For a ternary mixture that usually applies to the FRRPP reaction fluid, the Gibbs free energy of mixing (Altena and Smolders, 1982; Boom et al., 1994) is

$$\frac{\Delta G_M}{RT} = \sum_{i=1}^{3} n_i \ln \phi_i + g_{12} n_1 \phi_2 + g_{13} n_1 \phi_3 + g_{23} n_2 \phi_3, \tag{1.1.5}$$

where subscripts 1 and 2 indicate solvents, and subscript 3 represents the polymer.

The above-mentioned deficiencies of the Flory–Huggins theory can be alleviated, in part, by using the local-composition concept based on Guggenheim's quasichemical theory for the random mixing assumption and replacing lattice theory with an equation-of-state model (Prausnitz et al., 1986). More sophisticated models are available, such as the perturbed hard sphere chain (PHSC) and the statistical associating fluid theory (SAFT) (Caneba and Shi, 2002), but they are too mathematically sophisticated that they are impractical for subsequent computational efforts.

Modified Flory–Huggins equations used different techniques to account for the concentration dependence of χ or g without considering the true cause of the deficiency of the theory; thus, their accuracy to represent experimental data must

rely on a curve-fitting procedure. Even though they cannot generate a universal theory with a physical meaning, they represent the most practical methods to numerically characterize LCST behavior for realistic FRRPP systems (Caneba and Shi, 2002).

The Flory–Huggins equation is one of the simpler models in polymer systems to accurately predict the phase behavior of a real system. In its original version with constant interaction parameters, it cannot even predict the LCST, a common phenomenon in polymer systems. However, its simple form and requirement for less number of parameters make it very suitable for more complex systems. Furthermore, parameters in the Flory–Huggins equation can be made a function of composition or even molecular weight to account for the deviation from experimental data. Thus, the Flory–Huggins model is still very useful and one of the most frequently used methods for polymer systems.

1.1.1.2 Flory–Prigogine–Patterson Equation-of-State Theory

The importance of coupling liquid state properties with the adequate solution theory to take into account the volume, the intermolecular enthalpy, and the intermolecular entropy (i.e., the entropy exclusive of ΔS_{comb}), and in particular the changes of these extensive quantities undergo upon mixing becomes apparent. Early attempts to take account of liquid state characteristics in the treatment of solution proceed along two main lines (Flory, 1970): exploitation of the cell model as a basis for formulating the properties of liquid mixtures and application of corresponding states methods to selected classes of liquid mixtures (Prigogine, 1957). Further development is due to Flory by expanding the partition function of van der Waals form to the solution theory. This development uses the approach without the lattice superposition.

Prigogine (1957), using corresponding states ideas, first emphasized the importance of equation-of-state effects on solution thermodynamics. Later, Patterson and his coworkers (Patterson, 1968, 1982; Patterson and Delmas, 1970) used and extended these ideas to polymer solutions. The brief review of Patterson (1982) based on lattice theory of corresponding states ideas is briefed here to give an intuitive insight into the polymer solution behaviors. According to Patterson, the three contributions to the Gibbs free energy of mixing are the combinatorial or positional entropy of mixing, the intermolecular interaction arising from the different forces surrounding the molecules, and the free-volume effect. The first two components correspond to the original FH equation and lead to the UCST phenomenon. Compared to polymer–polymer or low molecular systems, the difference in free volume becomes very important for polymer–solvent system because of significant difference in size and shape between the components. For example, in a polymer solution where a polymer has similar chemical structure as the solvent, there is little dissimilarity in the intermolecular interactions but the free-volume difference is significant. In this theory, free-volume effects (entropic effects) also contribute to the interaction parameter χ besides the enthalpic contribution as used in Flory–Huggins theory (Patterson and Delmas, 1970). As temperature rises, the free volume of the solvent increases; however, the free volume of the polymer is nearly constant. Since

the difference in free volume increases with temperature, this eventually induces the incipience of LCST. For polymer/polymer systems, the contribution from free-volume difference is often negligible, and the LCST can be achieved only by some specific interactions between the components. Specific interactions contribute to the negative ΔG_{M} (or χ), whereas the dispersion forces or random dipole-induced dipole interaction always leads to a positive contribution to ΔG_{M} (or χ). The total χ along with its contributions from intermolecular interactions (dispersion forces and specific interactions) and free volume is graphically depicted elsewhere (Patterson, 1982).

The quantitative description of the above results may be made from the Flory EOS, or Prigogine–Flory theory, which originated from Prigogine's concepts and was developed by Flory (Patterson, 1982). It was based on the generalized van der Waals partition function:

$$Q = Q_{\mathrm{comb}}(\gamma v^*)^{N_{rc}}\left(\tilde{v}^{1/3}-1\right)^{3N_{rc}}\exp\left(-\frac{U_o}{kT}\right) \quad \text{with} \quad -\frac{U_o}{kT} = \frac{N_{rc}}{\tilde{v}\tilde{T}}, \tag{1.1.6}$$

where γ is a geometric constant; v^*, the hard-core volume per segment; $\tilde{v}$, reduced volume v/v^*; v, volume per segment; r, number of segments per molecule; T^*, characteristic temperature which reflects the potential energy between two segments; $\tilde{T}$, reduced temperature T/T^*, and c, Prigogine's parameter per segment. The corresponding equation of state is

$$\frac{\tilde{P}\tilde{v}}{\tilde{T}} = \frac{\tilde{v}^{1/3}}{\tilde{v}^{1/3}-1} - \frac{1}{\tilde{v}\tilde{T}}, \tag{1.1.7}$$

where $\tilde{P}$ is the reduced pressure, which is equal to P/P^*, and P^* is the characteristic pressure. Normally, V^*, T^* and P^* are obtained in the literature, or they can be estimated from other fluid properties.

1.1.2 Liquid–Liquid Phase Equilibria of Polymer Solutions

1.1.2.1 Binodal Equations

The binodal compositions or compositions of liquid phases α and β in equilibrium can be obtained by solving the following equations:

$$\Delta\mu_i^{\alpha} = \Delta\mu_i^{\beta} \quad \text{for all component } i = 1,2,3,\ldots,m, \tag{1.1.8}$$

wherein the chemical potential difference, $\Delta\mu_i$, is defined as

$$\Delta\mu_i \equiv \left(\frac{\partial \Delta G_{\mathrm{M}}}{\partial n_i}\right)_{T,P,n_{j\neq i}} \tag{1.1.9}$$

Based on Eq. (1.1.4) for ΔG_M, corresponding chemical potential expressions for a multicomponent system are

$$\frac{\Delta\mu_i}{r_k RT} = \frac{1}{r_k}(\ln\phi_k + 1) - \sum_{i=1}^{n}\frac{1}{r_i}\phi_i + (1-\phi_k)\left(\sum_{i<k}^{n-1} g_{ik}\phi_i + \sum_{j>k}^{n} g_{kj}\phi_j\right) - \sum_{i\neq k}^{n-1}\sum_{j\neq k, j>i}^{n}\phi_i\phi_j g_{ij}. \tag{1.1.10}$$

For a ternary system, Eq. (1.1.10) can be written for the components as

$$\frac{\Delta\mu_1}{r_1 RT} = \frac{1}{r_1}(\ln\phi_1 + 1 - \phi_1) - \frac{1}{r_2}\phi_2 - \frac{1}{r_3}\phi_3 + (1-\phi_1)(g_{12}\phi_2 + g_{13}\phi_3) - g_{23}\phi_2\phi_3, \tag{1.1.11}$$

$$\frac{\Delta\mu_2}{r_2 RT} = \frac{1}{r_2}(\ln\phi_2 + 1 - \phi_2) - \frac{1}{r_1}\phi_1 - \frac{1}{r_3}\phi_3 + (1-\phi_2)(g_{12}\phi_1 + g_{23}\phi_3) - g_{13}\phi_1\phi_3, \tag{1.1.12}$$

$$\frac{\Delta\mu_3}{r_3 RT} = \frac{1}{r_3}(\ln\phi_3 + 1 - \phi_3) - \frac{1}{r_1}\phi_1 - \frac{1}{r_2}\phi_2 + (1-\phi_3)(g_{13}\phi_1 + g_{23}\phi_2) - g_{12}\phi_1\phi_2. \tag{1.1.13}$$

1.1.2.2 Spinodal Equations

The spinodal curve for an m-component system is obtained when the determinant of the (m–1)-ranked second-derivative matrix of ΔG_M is zero. Thus,

$$\det\left[\frac{\partial^2\Delta G_M}{\partial\phi_i\partial\phi_j}\right]_{m-1} = 0. \tag{1.1.14}$$

The reason why only (m–1)th rank is considered is the existence of the so-called Gibbs–Duhem equation in thermodynamic systems.

For a binary polymer–solvent mixture, the spinodal equation reduces to

$$\frac{1}{RT}\frac{\partial^2\Delta G_M}{\partial\phi_P^2} = \frac{1}{r\phi_P} + \frac{1}{1-\phi_P} - \left[2\chi - (1-2\phi_P)\left(\frac{\partial\chi}{\partial\phi_P}\right) - \phi_P(1-\phi_P)\left(\frac{\partial^2\chi}{\partial\phi_P^2}\right)\right] = 0. \tag{1.1.15}$$

Here, r is the average degree of polymerization or polymer chain length, and Eq. (1.1.17) accounts for composition-dependent χ-parameter. If the χ-parameter is composition independent, Eq. (1.1.15) in turn reduces to

$$\frac{1}{RT}\frac{\partial^2 \Delta G_{\mathrm{M}}}{\partial \phi_{\mathrm{P}}^2} = \frac{1}{r\phi_{\mathrm{P}}} + \frac{1}{1-\phi_{\mathrm{P}}} - 2\chi = 0. \tag{1.1.16}$$

For ternary polymer (3)/solvent (2)/non-solvent (1) systems which apply to the FRRPP fluid systems, the spinodal equation becomes (Altena and Smolders, 1982)

$$\left(\frac{\partial^2 \Delta G_{\mathrm{M}}}{\partial \phi_2^2}\right)\left(\frac{\partial^2 \Delta G_{\mathrm{M}}}{\partial \phi_3^2}\right) - \left(\frac{\partial^2 \Delta G_{\mathrm{M}}}{\partial \phi_2 \partial \phi_3}\right)^2 = 0, \tag{1.1.17}$$

where

$$\frac{1}{RT}\frac{\partial^2 \Delta G_{\mathrm{M}}}{\partial \phi_2^2} = \frac{1}{\phi_1} + \frac{1}{v_2\phi_2} - 2g_{12} + 2g_{12}(u_1 - u_2) + u_1u_2\left(\frac{\partial^2 g_{12}}{\partial u_2^2}\right), \tag{1.1.18}$$

$$\frac{1}{RT}\frac{\partial^2 \Delta G_{\mathrm{M}}}{\partial \phi_3^2} = \frac{1}{\phi_1} + \frac{1}{v_3\phi_3} - 2g_{13} + 2u_2^2(1+u_1)\left(\frac{\partial g_{12}}{\partial u_2}\right) + u_2^3u_1\left(\frac{\partial^2 g_{12}}{\partial u_2^2}\right), \tag{1.1.19}$$

$$\frac{1}{RT}\frac{\partial^2 \Delta G_{\mathrm{M}}}{\partial \phi_2 \partial \phi_3} = \frac{1}{\phi_1} - g_{13} + \frac{g_{23}}{v_2} - g_{12} - u_1u_2\left(\frac{\partial g_{12}}{\partial u_2}\right) - u_1u_2^2\left(\frac{\partial^2 g_{12}}{\partial u_2^2}\right), \tag{1.1.20}$$

$$u_1 = \frac{\phi_1}{\phi_1 + \phi_2}, \tag{1.1.21}$$

$$u_2 = \frac{\phi_2}{\phi_1 + \phi_2}, \tag{1.1.22}$$

and if g_{13} and g_{23} are composition independent. Note that from an FRRPP standpoint, the solvent becomes the monomer, while the non-solvent becomes the precipitant.

A representative plot of binodal and spinodal curves for ternary polymer/monomer/precipitant systems (which is similar to that of a polymer/solvent/non-solvent system) is shown in Fig. 1.1.2 at constant temperature and pressure. The phase envelope pertains to the region encompassed by the binodal curves, in which there exist two phases at equilibrium. Outside the phase envelope is the single-phase region. The so-called tie lines are straight lines that join the binodal compositions at equilibrium. If the system has an LCST, then the size of the phase envelope increases with increasing temperature. If the system has a UCST, then the size of the phase envelope decreases with increasing temperature.

1.1.2.3 Measurement of Binodal and Spinodal Curves

A number of phase curve measurement methods have been used in conjunction with FRRPP studies. Some of them will be described in various sections throughout this monograph. Briefly, they include the following:

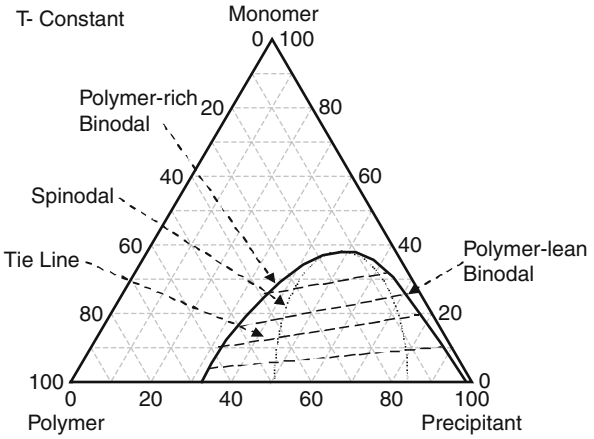

Fig. 1.1.2 Representative phase diagram in an equilateral triangular plot of a polymer/monomer/precipitant system showing binodal and spinodal curves and tie lines

1. Cloudpoint method, wherein the appearance and disappearance of another phase is detected through changes in turbidity of the fluid. Both binodal and approximate spinodal curves can be measured.
2. Time-resolved light scattering method, wherein the spinodal curve is measured based on vanishing mutual diffusivities.
3. Sorption method, wherein the spinodal curve is obtained when a swollen polymer membrane becomes incapable of further sorption due to vanishing mutual diffusivity.
4. Pulsed NMR method, which is used to determine binodal compositions based on differences in decay times of nuclear spins from polymer-rich and polymer-lean phases.

The cloudpoint method is the simplest and most reliable approach to measuring both binodal and spinodal curves. The cloudpoint apparatus is shown in Fig. 1.1.3. Usually, the method starts by loading the heavy walled tube container with the polymer and solvent. The temperature is raised to dissolve the polymer, at which point the solution is transparent. Then, the temperature is slowly changed until the mixture starts to appear cloudy. This indicates the formation of another liquid phase, and the onset of cloudiness can be interpreted as a spinodal point. To arrive at the binodal point corresponding to the fluid composition, the direction of temperature change is reversed until the mixture becomes clear again. The same measurement method is used for different compositions. However, for ternary polymer/monomer/precipitant systems, a more efficient method of traversing the phase diagram is used and presented in the next section.

Using the above-mentioned methods to measure phase curves, the following results are obtained for binary systems of interest. Figure 1.1.4 shows the result for polystyrene/cyclohexanol system, which has been a subject of early phase separation kinetics studies.

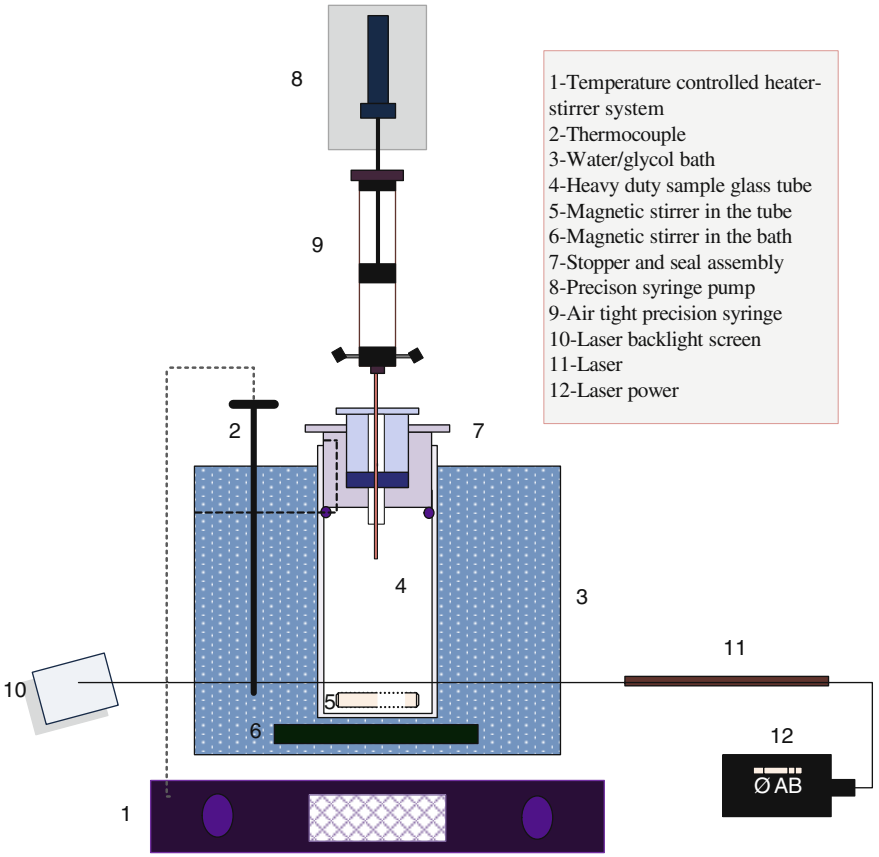

Fig. 1.1.3 Schematic experimental setup for generation of ternary phase diagrams using the cloudpoint method (Redrawn with permission from Wang et al., 1999)

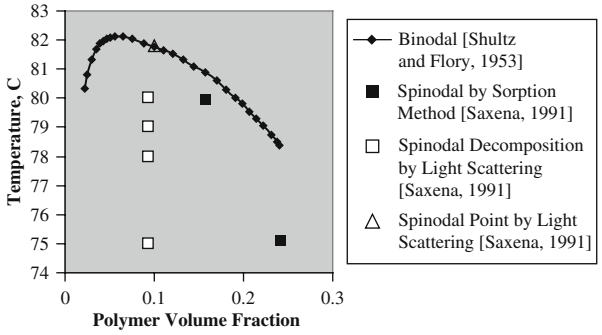

Fig. 1.1.4 Phase diagram-related results for polystyrene/cyclohexanol system

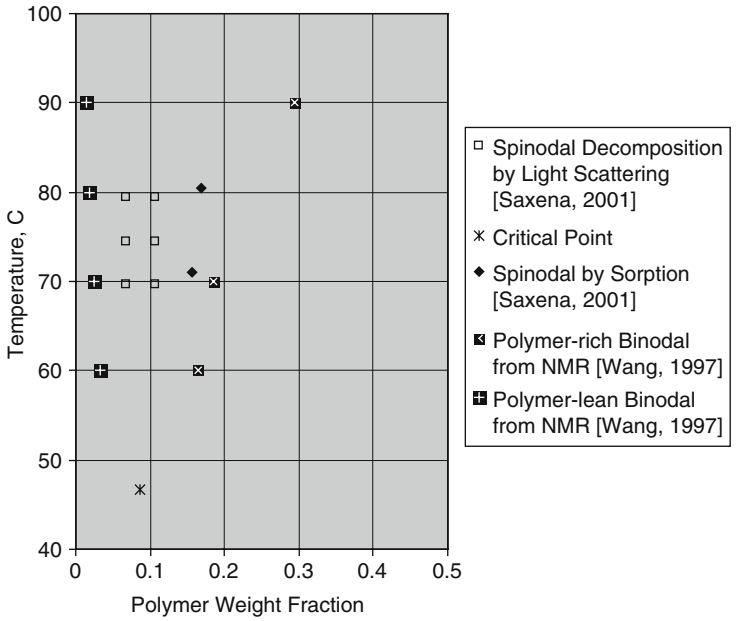

Fig. 1.1.5 Phase diagram measurement results for the PMAA/water system. The critical point (LCST) is obtained from the literature (Eliassaf and Silberberg, 1962). Spinodal decomposition-based points are used to analyze kinetics of phase separation deep inside the spinodal region

For the PMAA/water system that has become a prelude to studies of the PMAA/MAA/water reactive system, Fig. 1.1.5 shows phase curves and points that were obtained by our research group.

1.1.3 The LCST Phenomenon in Experimental Polymer/Small-Molecule Systems

Since it has not been easy to predict LCST data for polymer/solvent systems, an initial search was made for LCST data for mixed small-molecule systems. These were also considered "Universal" solvent systems, in which LCST behavior could be obtained with a wide variety of monomer/polymer systems. The following possibilities were obtained:

I. Mixed solvents – water/MEK, water/2-pentanone, water/other higher ketones, water/ethylene glycol methyl butyl ether, water/propylene glycol propyl ether, glycerol/guaiacol, glycerol/*m*-toluidine, glycerol/ethyl benzylamine, water/pyridines, water/piperidines (International Critical Tables, Volume III, 1928, pp. 386–398; Seidell and Linke, 1952)
II. Hydrocarbon gases – ethane, propane, and butane.

LCSTs have been known to occur 50–100°C below their critical temperatures (Freeman and Rowlinson, 1960; McHugh and Guckes, 1985).

Type I solvents form an LCST by themselves; they involve a variant of the currently understood FRRPP mechanism in polymer systems. As for Type II solvents, they offered good promise. It was believed that Freon® compounds are included in this class. The problem with these solvents is that they involve pressures in the 10–100 bar range.

1.1.3.1 LCST and the FRRPP Process

The free-radical retrograde-precipitation polymerization (FRRPP) process distinguishes itself from the conventional free-radical precipitation polymerization in both mechanisms and final product properties. In short, the FRRPP process proceeds above the LCST of the system, whereas the conventional-precipitation polymerization generally happens within the UCST region. For the different mechanisms of the UCST and LCST, one can expect that the polymerization process must be controlled by different schemes above the LCST and below the UCST. Furthermore, the product properties may possess some unique characteristics for the aforementioned reasons.

Since the discovery of the FRRPP process, research has been directed toward the study of the demixing polymerization mechanism (reaction kinetics, phase separation, morphology, product characterization, etc.). The FRRPP process relies heavily on the incipience of the LCST of the system. The fact that typical LCSTs of most nonpolar systems are much higher than normal operating temperatures for the free-radical polymerization process can make the FRRPP process infeasible. From a table that lists the LCST of polystyrene (PS) in some common solvents (Caneba, 1992a, b), the following observations and conclusions were drawn:

1. Most LCSTs lie between the boiling temperatures and the critical temperatures of the solvents, with notable exceptions for polystyrene in diethyl ether, acetone, and *t*-butyl acetate, wherein *T*/LCST (K/K) are 1.02, 1.03, and 1.08, respectively.
2. The similarities between the polarities and the shapes of the solvent and polymer have a significant effect on the LCST, and the more similar the polarities or the shapes of the solvent and the polymer, the higher the LCST.
3. The LCST has some relationship to the critical temperature of the solvent. The higher the critical temperature of the solvent, the greater the possibility that the system will possess a high LCST.

For the polystyrene/solvent systems listed (Caneba, 1992a, b), careful selection of the solvent(s) permitted the FRRPP process to be carried out at a relatively low temperature, which made this new polymerization method more promising. For high LCST systems, specially designed reactors can be used to carry out the FRRPP process. However the limitation is, the higher the temperature, the more likely the incipience of thermal degradation in the system. Additionally, running the free-radical

polymerization at relatively high temperature will result in more problems in process control, energy cost, and product quality. As far as the FRRPP process is concerned, the lower the LCST of the system, the easier the process control, and the better the product quality. Aqueous solutions of polar polymer systems could result in low LCST values. This makes FRRPP a very appropriate method for highly polar polymer systems, which can be at least be partially soluble in water. On the other hand, a few favorable cases, such as polystyrene–styrene–diethyl ether or polystyrene–styrene–acetone or polystyrene–styrene–*t*-butyl acetate, opened a new window for the application of the FRRPP process in nonpolar systems.

Efforts were also centered on the search for a practical solvent system that will exhibit an LCST with poly(methyl methacrylate) PMMA and poly(vinyl acetate) PVA. Results are recently being presented in the literature (Caneba et al., 2009). For the PVA/solvent system, no LCST data were reported in the literature, except for a citation on LCST behavior for partially hydrolyzed PVA in water. Cloudpoint experiments on PVA with mixtures of alcohol (ethanol, isopropanol, *n*-butanol, *t*-butanol) and water resulted in LCST behavior below 97ºC.

More recently, calculation of the LCST for polyethylene, polyvinylidene chloride, polychlorotrifluoroethylene, polystyrene, and polypropylene was undertaken using a theoretical method of atom connectivities for polymer and solvent (Liu and Zhong, 2005) (see Table 1.1.1). Some solvents of choice were water, butane, acetone, toluene, cyclopentane, *t*-butanol and methyl ethyl ketone, and THF. The LCST values for polyethylene, polyvinylidene chloride (PVDC), and polychlorotrifluoroethylene with the solvents are the same, because of the structure connectivity rules.

The determination of experimental LCST for the polymer–solvent mixtures was measured for PVDC–acrylonitrile (AN)–methyl methacrylate (MMA) 1 wt% in *t*-butanol; PVDC/AN/MMA 1 wt% in MEK; PVDC/AN/MMA 1 wt% in 50/50 wt% *t*-butanol/MEK mixture; PVDC/AN/MMA 1 wt% in 70% MEK/30% *t*-butanol mixture; polychlorotrifluoroethylene (PCTFE) 1 wt% in 70% MEK/30% *t*-butanol mixture; PVDC/VC in 70% MEK/30% *t*-butanol mixture; and polyvinyl methyl ketone

Table 1.1.1 LCST (*K*) values for various polymer/solvent pairs from theoretical calculations using connectivity rules (Liu and Zhong, 2005)

Solvent	Polyethylene	Poly(vinylidene chloride)	Polychlorotri-fluoroethylene	Polystyrene	Polypropylene
Water	361	361	361	–	–
Butane	386	386	386	–	429 (422)*
Acetone	396	396	396	352 (340)	–
MEK	401	401	401	357 (425)	–
Toluene	554	554	554	–	–
Cyclopentane	463	463	463	419 (428)	534 (540)
t-Butanol	436	436	436	–	–
THF	463	463	463	510 (552)	–

*Values in parentheses are experimental.

Table 1.1.2 LCST values of various polymers in azeotropic *t*-butanol/MEK

Polymer	LCST (°C)
PVDC–AN–MMA	112–123
PVDC–VC	105–114
PCTFE	97–107
PVMK	132–141

(PVMK) in 70% MEK/30% *t*-butanol. The PVDC/AN/MMA materials in *t*-butanol showed no cloudpoint transition, although PVDC/AN/MMA in MEK showed a cloudpoint of 145ºC. Further tests were done using mixtures of *t*-butanol and MEK to lower the cloudpoint from 145ºC. A test of 50/50% *t*-butanol and MEK showed no cloudpoint transition. A new set of experimental results using 70% MEK/30% *t*-butanol mixture is found in Table 1.1.2

1.1.3.2 Measurement of LCST-Based Ternary Phase Diagrams Using Cloudpoint Experimentation

Ternary (polymer/monomer/solvent) systems were investigated. The choice of the systems was based on the criterion that the systems should be suitable to run the FRRPP process.

Arbitrarily, the polymer/solvent system which has a relatively low LCST (i.e., LCST < 100ºC) is taken as the appropriate system to carry out the FRRPP process by using the corresponding monomer and free-radical initiator under moderate pressures. In practice, the FRRPP process should proceed at a temperature well above the LCST of the system to achieve a reasonably large two-phase envelope. Often, the molecular weight of the FRRPP polymer is not very high (as in solution polymerization), and this further requires a lower LCST system corresponding to the average molecular weight of the product. Usually, the aqueous polymer solution will give a LCST low enough to run the FRRPP process, and poly(methacrylic acid) (PMAA) polymerized in the water medium is chosen among these kinds of systems. For nonpolar polymer systems, the LCST is usually high and the appropriate system must be chosen to carry out the FRRPP process under suitable conditions. Polystyrene is one of the main commodity polymer products. The LCSTs of polystyrene in acetone and diethyl ether were cited to be equal to 67 and 42°C, respectively (Caneba, 1992a, b). Taking account of the actual molecular weight that can be achieved through solution polymerization under normal free-radical polymerization conditions, the styrene/diethyl ether system is the system that can display a significant phase envelope for the FRRPP process under 100°C and is mainly used in fundamental FRRPP efforts. Experiments show that both PMAA/MAA/water and polystyrene/styrene/diethyl ether systems have an applicable retrograde-precipitation behavior under the experimental conditions.

Materials

Methacrylic acid (MAA) was obtained from Aldrich Chemicals with 250 ppm inhibitor of methyl ethyl hydroquinone (MEHQ) without further purification. Styrene also came from Aldrich and was double distilled and inhibited with hydroquinone (HQ) before use. Diethyl ether (DEE) from Aldrich Chemicals was used as it is. Poly(methacrylic acid) (PMAA) made by the FRRPP process in our lab with different molecular weights and polydispersity indices (PDI) was used in the experiments. Polystyrene was bought from Pressure Chemicals Co. with different molecular weights and the same PDI of 1.06. The products through the FRRPP process in our lab were also used to determine the phase envelope.

Apparatus and Procedure

Ternary phase envelopes were determined with specially designed apparatus (Fig. 1.1.3) that consisted of a heavy-duty-wall tube with the outer diameter of 1.54 cm and effective length of 20.32 cm. Sometimes, a reference tube containing the solution with about the same polymer concentration of the sample, but with a composition in the homogeneous solution region, would also be used to double cross-check the cloudpoints. The sample tube had a tailored Teflon® stopper through which a channel with different diameters in different sections was cut to fit the requirement of a silicone rubber seal. The needle of a precision syringe could penetrate the silicone rubber without breaking the seal of the tube. Preweighed PS was transferred into the tube. The air in the tube was removed by vacuum before the experiment and the tube was mounted in the water bath. A small Teflon® coated magnetic stirrer was placed into the tube for stirring. The tube was capped with the specially designed Teflon® stopper and then subjected to vacuum. A clear water bath with magnetic stirrer was maintained within $\pm 0.1^{\circ}C$ of the required temperature. A syringe pump was used to accurately meter the solvents into the tube. A He–Ne laser beside the bath was installed to facilitate the determination of the end point. Small-molecule fluids (MAA, water, styrene, and DEE) could be added from the precision air-tight syringes into the tube to change the compositions of the mixture in the sample tube. The cloudpoint curve (CPC) was determined by adding a monomer (MAA or styrene) to the point of clarity of the turbid solution. The end point was determined by comparing the laser beam passing the solution in the sample or reference tube. For high concentration of polymer sample, the CPC was determined by static method, where known composition samples in sealed bottles (prepared from the knowledge of the phase boundary) were placed into an isothermal bath for trial-and-error experiments until some of the samples began to turn a little cloudy. Usually, three samples gave the approximate phase boundary for this method, but the error was larger than the method shown in Fig. 1.1.3. Also, precipitant (water or DEE) was added to the transparent sample until the sample began to turn opaque; or monomer (MAA or styrene) added to the opaque sample until it became transparent. However, this procedure was time consuming; thus, solvents and non-solvents were added at a reasonable rate. The so-called

instantaneous precipitation point curve (IPPC)[1] was obtained by adding precipitant (water or DEE) to the homogeneous solution of the sample tube until the solution became totally cloudy. For high polymer concentration samples, the IPPC can be determined by the static method described above, or by the method shown in Fig. 1.1.3 with more intense stirring. The accuracy of the air-tight precision syringe was ±0.01 ml with one drop of the liquid equal to around 0.002 ml.

Measurement of Tie Line Compositions

Ends of tie lines in phase diagrams intersect phase curves and represent compositions of phases in equilibrium. The procedure to measure tie line compositions started by placing known composition samples into the capped vials. Then, the vials were immersed into a constant temperature bath for at least 4 h (usually for about 8 h) to ensure the phase separation nearly completed. To separate the two phases in equilibrium, different procedures were used for the PMAA/MAA/water and PS/S/ether systems. For the PMAA system, samples were taken out of the bath and the polymer-lean phase was poured into aluminum pans. Weights of both phases were obtained right after the separation. Also, the weight of the polymer-lean phase could be obtained from the difference between the weight of the original sample and that of the polymer-rich phase. After that, both the polymer-lean and polymer-rich phases were dried completely. Finally, the weighed polymer samples were used to calculate the polymer concentrations in both phases. For the PS/S/ether system, the procedure was a little different. Due to the pressure in the vials, the polymer-lean phase was not obtained by the above method. Carefully designed caps for the small vials were used. The caps were designed such that the polymer-lean phase was taken out by syringe easily after the phase separation. Usually, the PS in the polymer-lean phase was negligible, and almost no dry solid polymer could be seen in the aluminum pan after drying within the experimental error. The weight of the polymer-lean phase was then obtained by the difference between the weight of the original sample and that of the polymer-rich phase.

After calculating the concentration of the polymer in both polymer-rich and polymer-lean phases, the phase diagram obtained from the cloudpoint experiment was constructed with the tie lines. From polymer concentrations in both phases, tie lines were drawn in the ternary phase diagram, which would meet with the overall composition of the starting fluid. If the three points were not in a straight line, results from the determination of binodal or the tie line experiment were not correct. Only data with nearly straight tie lines were reported for both systems.

[1] The IPPC is neither the binodal nor the spinodal, but the phenomenon happens within the spinodal envelope. In our experiment, the spinodal can only be approximated. But, the IPPC may play a very important role in practical situations. Before the system enters the IPPC from the corresponding CPC curve, it will remain partially cloudy without precipitation with stirring for a very long time. After the composition change brings the system into the IPPC region, it will precipitate even with the stirring. That means, the IPPC is the boundary whereby the real system begins to precipitate rapidly.

Results and Discussion

Most of the phase diagrams shown here pertain to the PMAA/MAA/water system. For the PS/S/DEE system, more extensive results are shown in Caneba and Shi (2002), and its phase envelope orientation looked similar to that in Fig. 1.1.2. Figure 1.1.6 shows the cloudpoint curves (CPC) for the PMAA/MAA/water system at different temperatures. When the temperature of the system was raised, the two-phase region was enlarged, which corresponds to the LCST phenomenon. Figure 1.1.7 shows phase diagrams of different PMAA molecular weight samples in the mixture of MAA and water. It is clear that the higher molecular weight sample will have a larger two-phase region. Experimental data in the high polymer concentration region (above 8 wt% of PMAA for systems investigated) were determined from the static method described earlier. Results showed that the monomer, MAA, was a very good solvent for PMAA and the two-phase region was still kept below 8% of monomer concentration even at 90°C. The CPC flattened out at the highest monomer concentration for a relatively broad polymer concentration region until the polymer concentration passed around 10 wt%. Then, the monomer concentration in the system along the CPC started to go down. As discussed in the section about the LCST behavior, due to the strong intra- and intermolecular interactions, the liquid–liquid phase behavior of this system is different from the nonpolar systems, where the LCST often occurs between the boiling point and the critical point of the solvent.

For the PMAA/MAA/water system, water is also a solvent for PMAA to a certain degree; thus, the phase behavior is different from non-solvent/solvent/polymer systems. On the other hand, inter- and intra-association effects accompanying the

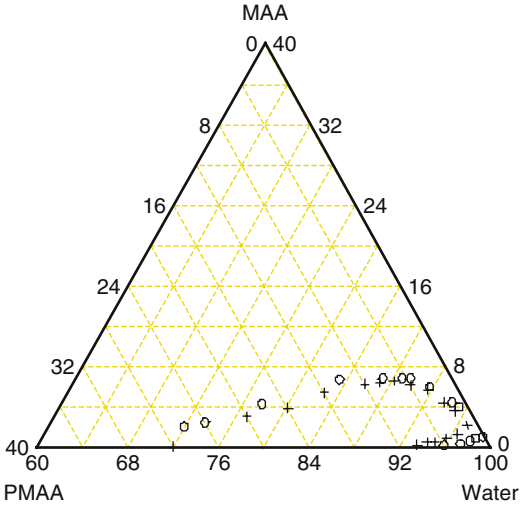

(M_n = 180,000 g/mol, *PDI* = 1.4; o: 90°C, +: 80°C)

Fig. 1.1.6 CPC (binodal points) of PMAA/MAA/water system at 80 and 90°C (Reproduced with permission from Shi, 1997)

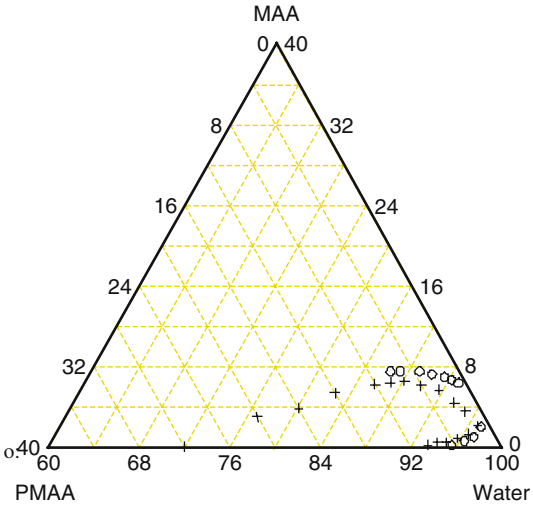

Fig. 1.1.7 CPC (binodal points) for PMAA/MAA/water systems of different PMAA molecular weights and at 80°C (Reproduced with permission from Shi, 1997)

(T = 80°C; + :M_n = 180,000, PDI = 1.4; o: M_n = 230,000, PDI = 1.41)

system make the liquid–liquid phase behavior more complicated. This was shown at the lower right corner of the ternary phase diagram where the CPC turns to the high polymer concentration again at a very low monomer concentration. This phenomenon is mainly attributed to the association effects between different components. In the vicinity of the pure water vertex when the polymer concentration is very low, the degree of the ionization of PMAA is relatively high, which is typically observed from a normal polyelectrolyte molecule. This enhances the solubility of the PMAA in water (Molyneux, 1984).

When MAA was added to such a system, the ionization of MAA was much stronger than that of PMAA, and the net effect was that the ionization of MAA prevented PMAA from ionizing in water. This changes the conformation of PMAA from expanded to a relatively compacted form, which in turn can reduce the solubility of PMAA in the system. If the monomer concentration in the system is high enough, the polymer will precipitate from the solution for the ionization suppression of the polymer molecules in water. This is the same as adding strong acid, such as hydrochloric acid, into the PMAA–water solution, which is often used to suppress the ionization of PMAA in water (Molyneux, 1984).

For PS/S/DEE systems, phase curves were measured by Wang (1997) at various temperatures and PS molecular weights. A replot of the data at 50 and 80°C at PS number average molecular weight of 25,000 g/mol is shown in Fig. 1.1.8. Note that Wang obtained tie lines that are horizontal for these systems. This means that both polymer-rich and polymer-lean phases have the same monomer composition at the same temperature. Based on the ternary Flory–Huggins equations (Eqs. 1.1.11–1.1.13), this corresponds to having the pairwise interaction parameter between S

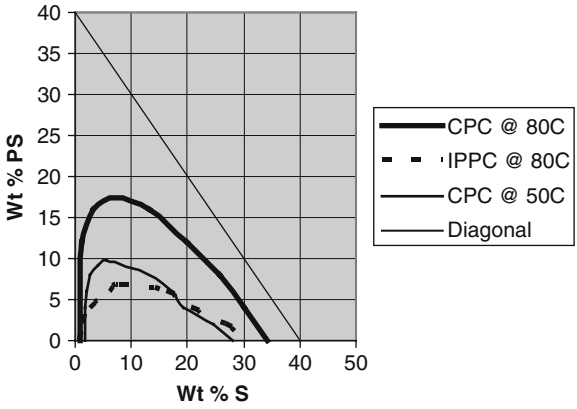

Fig. 1.1.8 Phase curves for LCST behavior of PS/S/DEE system. Note that tie lines should be considered horizontal, as verified experimentally

and PS to be approximately the same as the pairwise interaction parameter between S and DEE.

Figures 1.1.9–1.1.12 show more phase diagrams of the PMAA/MAA/water system. Figure 1.1.12 shows the CPC with several tie lines.

Figures 1.1.10–1.1.12 show the CPC and IPPC curves. For the system with PMAA number average molecular weight of 180,000 g/mol, the IPPC has been found to be very small. The spinodal curve is the theoretical boundary between the metastable and unstable regions, where the mutual diffusion coefficient is zero, whereas the IPPC corresponds to the sudden liquid–liquid phase separation under certain experimental conditions. The other difference is that the spinodal has a

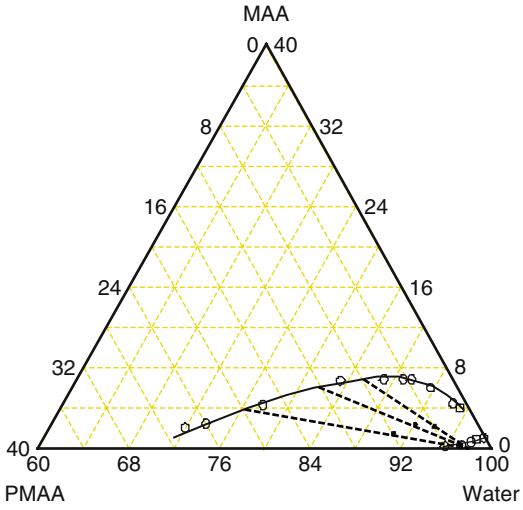

(PMAA: M_n = 180,000, PDI = 1.40; Temperature: 80°C)

Fig. 1.1.9 Phase diagram of the PMAA/MAA/water system at 80°C with tie lines (Reproduced with permission from Shi, 1997)